Sensitizers in extreme ultraviolet chemically amplified resists: mechanism of sensitivity improvement

Yannick Vesters
Jing Jiang
Hiroki Yamamoto
Danilo De Simone
Takahiro Kozawa
Stefan De Gendt
Geert Vandenberghe

SPIE.

Sensitizers in extreme ultraviolet chemically amplified resists: mechanism of sensitivity improvement

Yannick Vesters,[a,b,*] **Jing Jiang,**[a] **Hiroki Yamamoto,**[c,d] **Danilo De Simone,**[a] **Takahiro Kozawa,**[c] **Stefan De Gendt,**[a,b] **and Geert Vandenberghe**[a]
[a]IMEC, Leuven, Belgium
[b]KU Leuven, Department of Chemistry, Leuven, Belgium
[c]Osaka University, Institute of Scientific and Industrial Research, Osaka, Japan
[d]National Institutes for Quantum and Radiological Science and Technology, Takasaki, Japan

Abstract. Extreme ultraviolet (EUV) lithography utilizes photons with 92 eV energy to ionize resists, generate secondary electrons, and enable electron driven reactions that produce acid in chemically amplified photoresists. Efficiently using the available photons is of key importance. To increase photon absorption, sensitizer molecules, containing highly absorbing elements, can be added to photoresist formulations. These sensitizers have gained growing attention in recent years, showing significant sensitivity improvement. Aside from an increasing absorption, adding metal salts into the resist formulation can induce other mechanisms, like higher secondary electron generation or acid yield, or modification of the dissolution rate that also can affect patterning performance. In this work, we used different sensitizers in chemically amplified resists. We measured experimentally the absorption of EUV light, the acid yield, the photoelectron emission, the dissolution rate, and the patterning performance of the resists. Addition of a sensitizer raised the acid yield even though a decrease in film absorbance occurred, suggesting an apparent increase in chemically resonant secondary electrons. While patterning results confirm a significant sensitivity improvement, it was at the cost of roughness degradation at higher sensitizer loading. This is hypothesized by the chemical distribution of the sensitizer in the resist combined with a modification of the dissolution contrast, as observed by dissolution rate monitor measurements. © 2018 Society of Photo-Optical Instrumentation Engineers (SPIE) [DOI: 10.1117/1.JMM.17.4.043506]

Keywords: extreme ultraviolet lithography; chemically amplified resist; metal sensitizer; acid yield; dissolution rate.

Paper 18077 received Jun. 21, 2018; accepted for publication Nov. 14, 2018; published online Dec. 12, 2018.

1 Introduction

Conventional understanding of the light–matter interaction during exposure of chemically amplified photoresist by extreme ultraviolet (EUV) radiation is as follows:[1,2] the 92-eV EUV photons are absorbed by the atoms composing the photoresist initiating an ionization process that ejects a photoelectron. These primary electrons travel through the material and thermalize, losing energy through inelastic scattering processes, including the generation of secondary electrons. At a resonant energy, the cascading electrons of lower energy interact with the photo-acid generators (PAG) in their vicinity, leading to the generation of acids.

After exposure, a bake step allows the acid generated to diffuse and catalyze a deprotection reaction on functional groups of the photoresist polymer. This reaction leads to a change of hydrophilicity of the polymer, and therefore a solubility switch between exposed and nonexposed resist. Subsequent selective development is then possible in an aqueous-based developer.

As the number of photons per unit dose reduces relative to longer wavelengths and the resist volume diminishes when patterning features of smaller critical dimension, stochastics[3] become an inevitable concern, because information transfer from the mask is lost and blurred. Efficiently using the available photons is of key importance to promote sensitivity without loss of image fidelity.

Unlike DUV lithography, where absorbed photons directly excite specific photoactive molecules, photons at 92 eV can ionize all atoms, though specific elements have a significantly higher atomic photon-absorption cross-section at EUV wavelength, and these values are reported in Ref. 4.

Therefore, adding molecules with highly absorbing elements to photoresist formulations can sensitize the material, reducing the required exposure dose without loss of information and maintenance of image quality. These types of sensitizers have received growing attention in recent years and significant sensitivity improvement has been reported.[5] Nevertheless, there are little experimental evidences that the sensitivity improvement is due to the higher absorption only. Indeed, adding metal salts into the resist formulation can induce other mechanisms like modification of the dissolution rate, potentially also affecting patterning performances.[6]

In this work, we first want to verify that addition of sensitizer translates consistently into a measured absorption increase.

Further, it is known that a higher acid generation leads to higher sensitivity,[7] so we intend to confirm that a photoresist that absorbs more EUV photons because of sensitizer addition, effectively generates a proportionally higher acid concentration.

Finally, dissolution characteristics for the sensitized photoresist formulations are examined.

In this paper, we report the results of two different photoresist platforms, where alkaline earth organometal salts were

*Address all correspondence to Yannick Vesters, E-mail: yannick.vesters@imec.be

added. Sensitivity improvement was observed when patterning line-space features. To better understand the mechanism underlying this sensitivity improvement, further experiments were performed:[8] acid yield measurement, photoelectrons emission measurement and dissolution rate measurement by dissolution rate monitor (DRM), and quartz crystal microbalance (QCM) method.

2 Materials and Methods

2.1 Photoresist Film Preparation

Two photoresist platforms were used in this study, as described in Table 1. Resist NXE1631 was mixed with sensitizer A in two different loadings. Resist NXE1716 was mixed with sensitizer B in three different loadings. Both sensitizers are proprietary salts composed of an organic anion ionically bonded to an alkaline earth metal in its M^{2+} cationic state. For sensitizer B, the alkaline earth metal is magnesium, chosen due to its high absorption cross-section of 1.49×10^5 cm^2/g (at 91.5 eV), which is five times higher than carbon.[4] Sensitizer A is a heavier atom from the same group. Using the elemental composition of the sensitizers, the loading, and the tabulated values of absorption cross-section, it is possible to calculate the theoretical absorption increase due to the addition of sensitizer, assuming constant density (Table 1). However, it is likely that the density of the photoresist is impacted by the sensitizer addition.

Spin coating was performed with spin speed in the range of 1000 to 1500 rpm and followed by a 60 s postexposure bake (PEB) at 105°C for platform A and 90°C for platform B. Different dilutions of the photoresist in casting solvent were needed to reach 100-nm film thickness (for acid yield measurement and QCM) and 30- to 40-nm film thickness (for patterning test, absorption measurement, photoemission measurement, and DRM measurements).

2.2 Patterning Performance Upon EUV Exposure

For each lithography test, on a TEL LITHIUS Pro Z track, 35 nm of the resist was coated on 20 nm AL412 (Brewer Science, Inc.) underlayer. Exposure was made on IMEC's

Table 1 Material description and increase of theoretical absorption coefficient at 91.6 eV.

Sample name	Reference platform	Added mol of sensitizer per g of resist	Theoretical absorption (α) increase[a]
A_0	NXE1631	0	α_A
A_{Low}	NXE1631	$8.8 \pm 0.1 \times 10^{-5}$	$\alpha_A + 1.3\%$
A_{High}	NXE1631	$13.8 \pm 0.1 \times 10^{-5}$	$\alpha_A + 1.8\%$
B_0	NXE1716	0	α_B
B_{Low}	NXE1716	$3.6 \pm 0.1 \times 10^{-5}$	$\alpha_B + 0.7\%$
B_{High}	NXE1716	$11.0 \pm 0.1 \times 10^{-5}$	$\alpha_B + 2.1\%$
$B_{VeryHigh}$	NXE1716	$36.6 \pm 0.2 \times 10^{-5}$	$\alpha_B + 6.8\%$

[a]Calculated using CXRO database[9] assuming constant density.

ASML full-field scanner NXE3300B with dipole 90X illumination (sigma inner/outer: 0.62/0.90). TMAH 0.26 N was used as developer and SPC683 (Merck KGaA) rinse was applied after PEB (90°C, 60 s). The target feature was 44-nm pitch and 22-nm lines with no reticle bias. Focus-exposure matrix was imaged to determine the dose-to-size of the samples based on top-down scanning electron microscope (CD-SEM) measurement. These were performed on HITACHI CG-5000 tool with beam settings at 500 V and 8 pA. Images are 1024×1024 pixels with a rectangular scan and have a field-of-view of 0.9 μm $\times$ 2.755 μm. The roughness values come directly from the CD-SEM software, and no noise correction was applied (SEM biased values).[10]

2.3 EUV Absorption Measurement

Absorption at EUV wavelength was measured in Elettra synchrotron (Trieste, Italy) using a calibrated photodiode. The photoresist films were spin-coated and baked on a wafer coupon with 30-nm silicon nitride deposited on Si. Then, the Si wafer was etched back, to end up with a free-standing SiN membrane coated with photoresist. Transmission of the coated membrane was then measured, and absorption coefficient α of the photoresist layer was calculated using

$$T_{Measured}(\lambda) = T_{SiN}(\lambda) \times T_{PR}(\lambda) = e^{(\alpha_{SiN} d_{SiN} + \alpha_{PR} d_{PR})}, \quad (1)$$

$$\alpha_{SiN} = -\frac{4\pi}{\lambda} k_{SiN}, \quad (2)$$

where T is the transmission, λ is the wavelength, d is the thickness of the layer, and k is the extinction coefficient with the SiN index referring to the SiN membrane and the PR index to the photoresist film. Absorption of the SiN was previously calculated from measurement of the SiN membrane only. Details about the method used for these transmission measurements can be found elsewhere.[11–13]

2.4 Photo-Emission Measurement

Photo-emission of the photoresist sample during exposure to 13.5-nm light was measured at the Elettra synchrotron (Trieste, Italy). Samples were placed onto a conductive sample holder connected to a Keithley picoammeter. During exposure to a known light intensity (using calibrated photodiode), electrons are emitted from the photoresist surface to the vacuum chamber, and a drain current flows from ground to the sample to neutralize the holes generated. The photo-emission is calculated from the measured drain current divided by the number of incident photons obtained from the diode. Details on the setup can be found elsewhere.[12–14]

2.5 Acid Yield Measurements

Acid yield measurements were made at Osaka University using the following photometric method: Coumarin 6 (C6, Aldrich Chem.) was used as an indicator to evaluate the acid yield.[15,16] About 5 wt% C6 was added to the photoresist formulation. The resulting solutions were spin-coated on 3-in. quartz wafer. After coating, the films were exposed to EUV radiation (Energetic, EQ-10M). Absorption spectra were recorded using a JASCO V-670 spectrophotometer to quantify the acid yield in thin sample films by measuring

the characteristic absorption of the protonated form of C6 (533 nm). The experimental procedure has been reported in detail elsewhere.[17,18]

2.6 Dissolution Rate Monitor Measurements

Dissolution rate of the resist was measured using IMEC custom-build DRM tool. Photoresist was coated onto 300-mm Si wafer above a 1000 nm thermally grown SiO_2 layer. Resist was exposed to flood EUV light on ASML NXE3300 scanner. After exposure and PEB, the wafer is brought to the DRM tool for dissolution rate measurement: Photoresist is put in contact with the developer solution (TMAH 0.26 N), while thickness is measured dynamically by reflectometry, as further described in Ref. 19.

2.7 Quartz Crystal Microbalance Measurements

QCM measurement was performed at Osaka University. Dissolution behavior of resist with and without sensitizer was investigated by using the QCM-based analyzer (Litho Tech Japan RDA-Qz3). The photoresist films with and without sensitizer were spin-coated onto a quartz crystal. Resist film thickness was measured with a spectroscopic ellipsometer. The films were exposed to EUV radiation (Energetic, EQ-10M). After exposure, they were baked at 90°C for 60 s. The exposed films were subjected to QCM analysis in TMAH developer solvents. After development, they were rinsed in water before drying. Detail about the procedure can be found in Ref. 20.

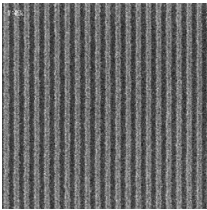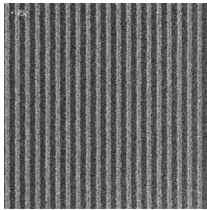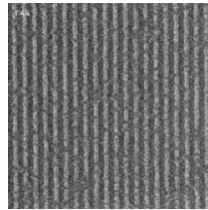## 3 Results and Discussion
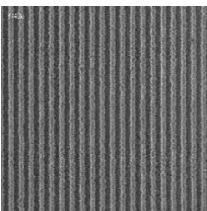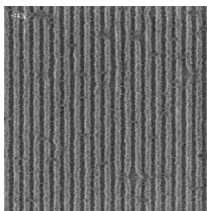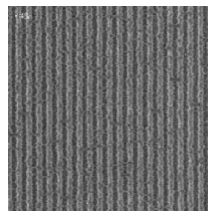
3.1 Patterning Performance

The resists were patterned with NXE3300 scanner. Results of line:space dense patterning at 44-nm pitch are presented in Fig. 1.

We observe a significant dose reduction in presence of the sensitizer. The dose-to-size is reduced by 31% for A_{Low} and 37% for A_{High}, while for the B platform, sensitivity was improved by 14% for B_{Low} and 27% for B_{High}.

At high sensitizer loading, we observed a clear degradation of the pattern quality for both platforms. Nevertheless, addition of a sensitizer does not necessarily lead to pattern degradation, as visible in the case of A_{Low}, where the line-width roughness was reduced compared to the reference. This shows that an optimized loading of sensitizer can lead to a simultaneous reduction of dose and roughness at identical resolution. Nevertheless, apart from A_{Low}, the reduction in dose for the other samples is combined with a degradation of the pattern (higher LWR, line breaks).

Additionally, the dose response is not linear with sensitizer loading: the loading in A_{Low} is ⅔ of A_{High} but the sensitivity impact is relatively similar. On the opposite, loading in B_{Low} is ⅓ of B_{High} but the reduction is half.

Furthermore, the reduction in dose experimentally observed is up to 30%, whereas the theoretical absorption (see Table 1) is increased by only a few percent. To understand where this discrepancy comes from, experimental evaluation of the resist absorption was performed.

Sample	A_0	A_{Low}	A_{High}
Picture HP 22nm			
Dose-to-size (mJ/cm²)	16.0	11.0	10.0
Dose reduction	ref	- 31 %	-37%
LWR (nm)	7.4 ±0.3	6.5±0.3	9.2±0.5
Sample	B_0	B_{Low}	B_{High}
Picture HP 22nm			
Dose-to-size (mJ/cm²)	11.0	9.5	8.0
Dose reduction	ref	-14%	-27%
LWR (nm)	6.7±0.3	9.4±0.5	10.3±0.5

Fig. 1 Patterning performance of the samples exposed on NXE3300. LWR values as measured by CD-SEM.

3.2 Absorption Measurement

The absorption of the resists at EUV wavelength obtained through transmission measurements is reported in Fig. 2. Even though the sensitizer salts for both platforms were selected based on their high absorbance cross-section, each showed a reduction in the measured absorption of EUV light with an increase of sensitizer loading.

While the sensitizer salt was blended with the photoresist to increase its absorption, the data presented show an opposite trend for the two sensitizers tested, with a lower absorption coefficient in presence of the sensitizer compared to the reference sample (resist only).

A first hypothesis to explain this result is that the addition of an ionic salt in a polymer blend could change the density (by inducing more free volume between the hydrophobic polymer chains). For the calculated absorption, a constant density was assumed. As absorption is proportional to density, a less dense material would translate in a lower absorption coefficient. This could account for most of the absorption loss observed.

An additional hypothesis could relate to the fact that the absorption cross-section used for the theoretical calculation of the absorption coefficient is based on the pure element. In our case, however, both sensitizers are ionic salts and the metal atoms used are in their cationic state (X^{2+}), bound to an anion. It is known that the chemical environment (or oxidation state) of a metallic atom can lead to a shift of its X-ray absorption edges by several eV.[21] In the case of sensitizer B, the L_I absorption edge of metallic Mg is 88.6 eV.[4] Therefore, a shift due to the chemical environment (Mg^{2+} instead of Mg) could induce a deviation from the theoretical Mg absorption cross-section at 92 eV. This would translate in a reduced absorption for the bounded Mg^{2+} in sensitizer B.

The absorption coefficient α increase expected with addition of sensitizer (Table 1) would thus be reduced, and this combined with a density decrease can explain the trend observed in Fig. 2.

In any case, the measured absorption was decreased for the sensitized resist, even though the sensitivity on patterned
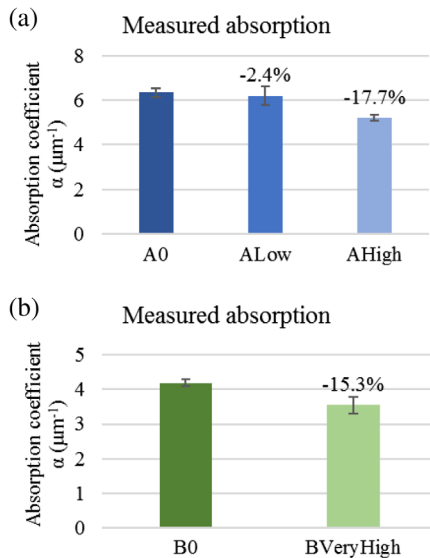
wafer was increased. It is necessary to understand how this situation is possible, and therefore, the acid yield of these samples upon exposure to EUV was measured.

3.3 Acid Yield Measurement

As the improvement in sensitivity does not arise from the increased absorption of the resist, it could come either from the mechanisms following photon absorption or from nonexposure related mechanisms like dissolution changes. To verify this, the amount of acid generated at the end of the exposure step was measured using the dye method.[17] The acid generated at three different exposure doses was measured by adding C6-dye to four samples of each platform (A and B): the photoresist without sensitizer, with a low sensitizer loading, with a high sensitizer loading, and a control sample containing only the polymer and a low loading of sensitizer (neither PAG nor quencher). The results are presented in Fig. 3.

Across dose, an average of 14% increase of acid yield for A_{Low} and up to 66% increase for A_{High} was observed compared to the nonsensitized A_0 sample. Similarly, B_{Low} and B_{High} acid yield increased by an average of 35% and 66%, respectively, compared to B_0.

Apart from A_{Low}, these numbers are in line with the sensitivity improvement observed: higher acid yield is achieved, and the increased acid amount quantitatively explains the dose-to-size reduction observed.

As an acid yield increase was observed at all doses when a sensitizer is added to the photoresist blend, we wondered if
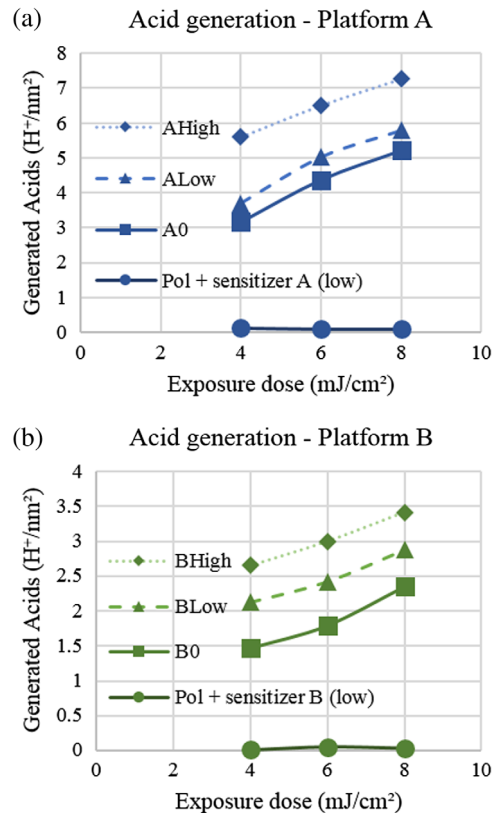
Fig. 2 Experimentally measured absorption coefficient for the resist platform with (a) sensitizer A and (b) sensitizer B.

Fig. 3 Measured generated acid as a function of the exposure dose, with four samples for each platforms (a) A and (b) B: resist with no sensitizer, with low and with high sensitizer loading, and resist with low sensitizer loading but without PAG and quencher (polymer only).
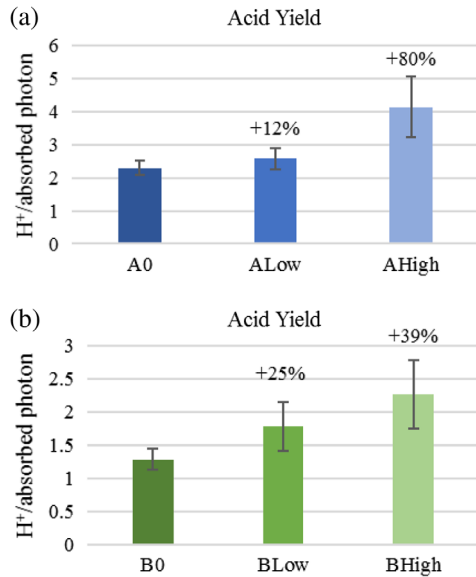
Fig. 4 Acid yield expressed in proton per absorbed photon: (a) platform A and (b) platform B at different sensitizer loading.

the sensitizer itself was playing the role of a photo-acid generator: the metal cation could break the ionic bond with the anion upon exposure, and the anion would capture a proton from the polymer matrix. This hypothesis can be disproved as no acid was generated for the control sample composed of the polymer + sensitizer (without PAG and quencher). The sensitizer is thus not acting as a PAG by itself.

Using the measured absorption coefficient, the above data were translated into number of acids generated per absorbed photon. Considering that in these resists, a quencher is present, and a portion of the acid produced upon exposure is quenched before being probed by the acid dye. The remaining number of acid molecules generated by a single EUV photon in the photoresists with and without sensitizer is shown in Fig. 4. As the amount of acid generated in the film is higher in the presence of sensitizer, as the measured absorption is lower, we logically observe a significantly higher yield of acid generated per absorbed photon.

As the sensitizer does not increase the absorption of photons, it means that the presence of sensitizer helps achieving higher PAG conversion to acid. Two possible explanations for this phenomenon are that the presence of an ionic salt near a PAG facilitates the reaction leading to acid generation or that the addition of sensitizer increases the secondary electron generation. This second hypothesis was tested by performing photo-emission measurements.

3.4 Photo-Emission Measurement

We measured the photo-emission of the samples under EUV exposure. The results are presented in Table 2.

While A_{Low} does not see a significant change in terms of photoemission, the presence of sensitizer for A_{High} leads to an increase of about 3.5% of the electron emission. For platform B, the presence of sensitizer showed a clear increase of about 17% of the electrons emitted for $B_{VeryHigh}$ (other conditions were not tested).

Based on the previous evidence, it was shown that the introduction of sensitizer into the photoresist likely

Table 2 Photo-emission measurement at 91.6 eV.

Sample	Measured photo-emission (emitted e− per incident photon)
A_0	$28.9 \pm 0.38 \times 10^{-3}$
A_{Low}	$28.6 \pm 0.38 \times 10^{-3}$
A_{High}	$29.9 \pm 0.39 \times 10^{-3}$
B_0	$19.3 \pm 0.23 \times 10^{-3}$
$B_{VeryHigh}$	$22.6 \pm 0.25 \times 10^{-3}$

helps to generate more secondary electrons that efficiently reacts with PAG to increase acid yield. This mechanism partially explains the sensitivity improvement observed, especially for the case of sensitizer B. For sensitizer A, the significant dose reduction observed with A_{Low} cannot be explained by the secondary electron generation, and therefore additional mechanisms likely play a role. In that perspective, the impact of sensitizer on dissolution properties was investigated.
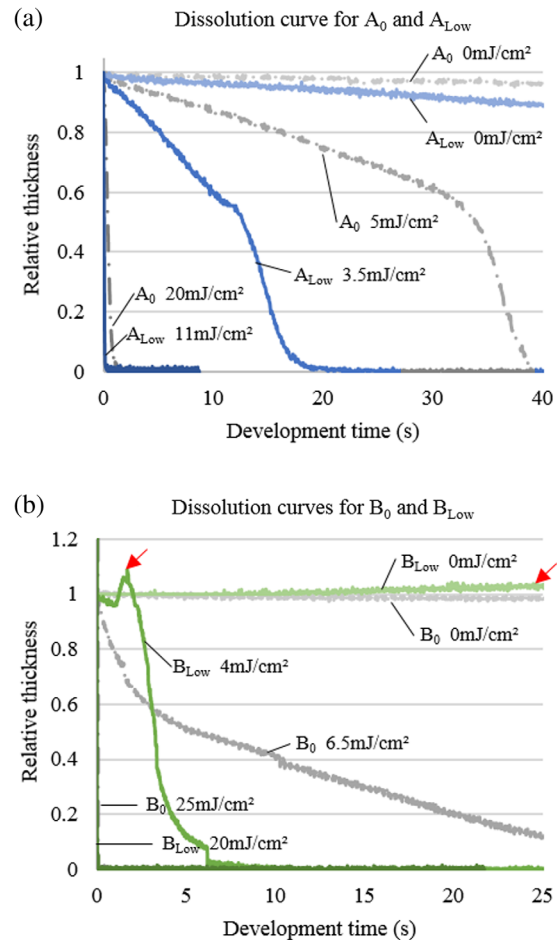
Fig. 5 Evolution of the film thickness when the photoresist (with and without sensitizer) is in contact with the developer, for unexposed resist, partially exposed resist and totally exposed resist. (a) Platform A and (b) platform B.
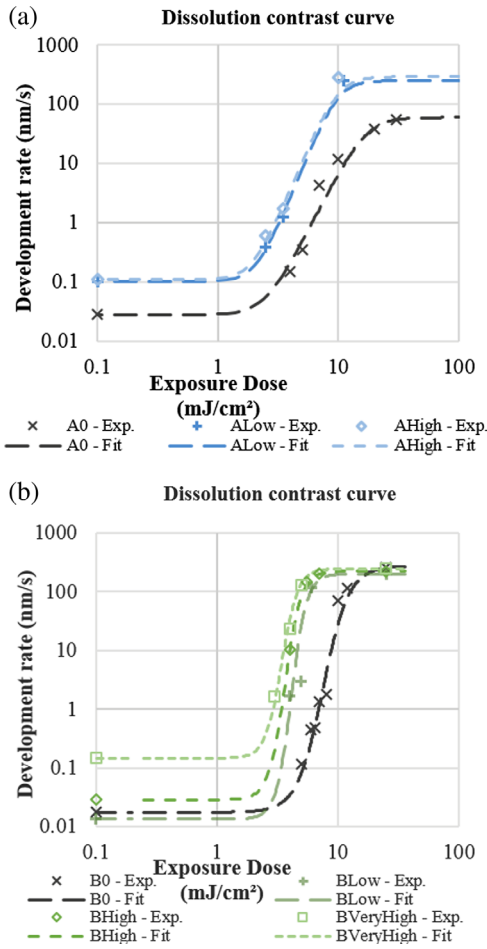
Fig. 6 Development rate as a function of exposure dose, measured by DRM (a) for platform A and (b) platform B with various sensitizer loading. The experimental data points were fitted using the Original Mack model.[22]

3.5 Dissolution Properties

To better explain the pattern degradation observed (cf Fig. 1) in case of sensitizer addition, the dissolution rate of the resist was measured using DRM at various exposure doses. The most representative dissolution curves are plotted in Fig. 5. For sensitizer A, we see that the presence of the metal salt (polar compound) increases the dissolution rate, for unexposed as well as for exposed resist. This is explained by the fact that we introduce a hydrophilic compound in the photoresist formulation, and thus, aqueous development is facilitated. This increased dissolution rate for both resist platforms contributes also partially to the sensitivity improvement observed with the addition of a sensitizer.

In addition, for sensitizer B, we observe a swelling of the photoresist in unexposed and partially exposed film [Fig 5(b), arrows]. This is likely due to the facilitation of the penetration of water into the film due to the metal salt, together with a solvation of the salt.

From these curves, average development rates were calculated and are reported as a function of the exposure dose in Fig. 6. These dissolution contrast curves show a significant impact of the addition of sensitizer. For A_{Low} and A_{High}, dissolution rate of unexposed resist is three times higher compared to A_0. Fully exposed resist development rate is increased nearly five times. As a result, the total contrast is increased compared to A_0, by 27% for A_{Low} and by 37% for A_{High}.

In the case of sensitizer B, the minimum development rate is also increased by the presence of sensitizer. But in this case, the maximum development rate is not significantly impacted. For this reason, the contrast between development rate of exposed and unexposed resist decreases drastically with the loading of sensitizer.

As a higher contrast is usually correlated with better patterning performances, this contrast difference between A and B explains why the roughness of the patterning with platform B is degraded at all loading while there is an optimum loading leading to roughness improvement for platform A.

Furthermore, as the presence of sensitizer increases the dissolution rate, the local concentration variability induced by the chemical distribution of the sensitizer molecules in the polymer matrix leads to variability of the local dissolution rate, contributing to higher roughness and pattern degradation during development.

In addition to the DRM measurement, QCM measurement was also carried out on platform A. The relationship between resist thickness and development time was obtained in photoresist with and without sensitizer, as shown in Fig. 7.
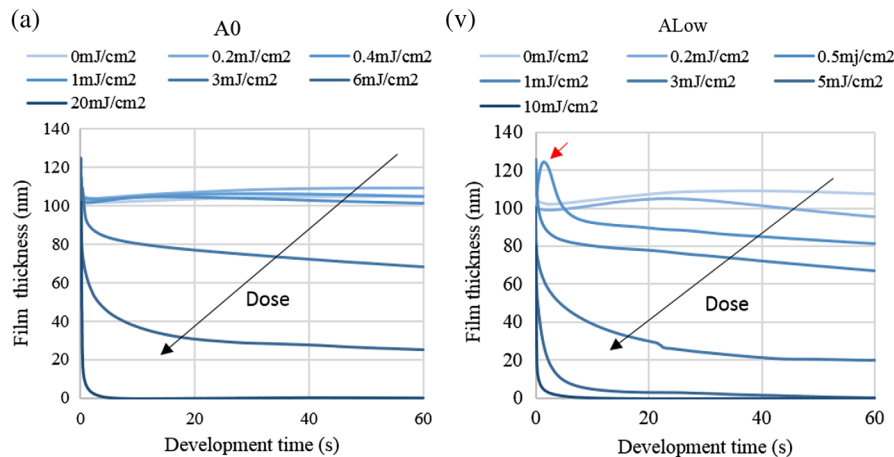
Fig. 7 QCM measurement of the thickness during development for (a) sample A_0 without sensitizer and (b) A_{Low} with sensitizer. We observe swelling in the presence of sensitizer for low exposure doses.

Swelling of the photoresist in unexposed and partially exposed film with very small dose was observed in photoresist with sensitizer [Fig. 7(b), arrows]. Furthermore, the development rate of A_{Low} is faster than A_0, which is consistent with DRM measurement. This is due to higher acid yield of A_{Low} compared to A_0 due to the presence of the metal salt.

4 Conclusion

Adding metal sensitizer to CAR photoresist is proposed as a potential solution to the RLS requirement challenge. As shown in this paper, it is possible to improve RLS performance of a photoresist by selecting properly a sensitizer and optimizing its loading: one sample (A_{Low}) indeed showed an improvement of dose of 30% simultaneously with a reduction of roughness due to the addition of sensitizer. Nevertheless, in most cases, the addition of sensitizer induces a roughness increase simultaneously with the dose reduction.

With this paper, we demonstrated that the mechanisms leading to this performance improvement are multiple. First, we have shown that the sensitivity improvement by sensitizer does not have originate from a higher EUV photon absorption. Indeed, in our case, sensitizer addition resulted in a reduction of the absorption of the resist under our experimental conditions. Instead, the sensitivity improvement is due to a higher conversion of the photons into acid in presence of sensitizer, notably due to a higher secondary electron generation. This increased efficiency is the first mechanism to explain the sensitivity improvement.

Second, the addition of ionic salts to a photoresist blend impacted the dissolution properties, specifically by increasing the development rate of the resist, contributing to the reduction of the dose-to-size of the resist. This second mechanism also contributes to the sensitivity improvement observed with sensitizer addition.

Furthermore, the modification of the dissolution properties impacts the contrast of the resist, potentially detrimental to the patterning. Indeed, if the contrast is lowered, the local variation of sensitizer concentration can be at the origin of the degradation of the patterning (roughness, line breaks) observed at high sensitizer loading. This degradation can be due to the nonuniformity of the sensitizer distribution combined with the two effects described in this paper: higher acid generation around the sensitizer molecule and higher dissolution rate, which would both lead to a higher local variability and thus increased roughness.

As the observed sensitivity improvement was shown to originate notably from the higher electron generation and acid yield, it shows that these phenomena can be modulated by blending specific molecules in the resist formulation. This opens engineering possibilities to control electron and acid blur.

It is also interesting to observe that the only sample (A_{Low}) showing simultaneous dose reduction and roughness improvement is the sample showing less impact on photon absorption, electron generation, and acid yield compared to the other samples. For all samples showing a significantly higher electron generation and acid yield, roughness was also increased. This shows that the sensitizers tend to act as amplifier of a noisy signal if they do not primarily increase photon absorption. In our opinion, a good sensitizer must increase the absorption of the resist. Therefore, we recommend including experimental absorption measurement when screening sensitizer candidates, as relying on theoretical absorption values can be misleading, as shown in this paper.

Further, the sensitizer should have as little impact as possible on the dissolution rate of the resist drastically. Therefore, nonionic species would be preferred. Last, the sensitizer should be distributed as uniformly as possible, and covalently bonding the sensitizer to the polymer backbone would be the most effective way to achieve this goal.

References

1. T. Kozawa and S. Tagawa, "Radiation chemistry in chemically amplified resists," *Jpn. J. Appl. Phys.* **49**(3), 030001 (2010).
2. D. De Simone, Y. Vesters, and G. Vandenberghe, "Photoresists in extreme ultraviolet lithography (EUVL)," *Adv. Opt. Technol.* **6**(3–4), 163–172 (2017).
3. P. De Bisschop, "Stochastic printing failures in extreme ultraviolet lithography," *J. Micro/Nanolithogr. MEMS MOEMS* **17**(4), 041011 (2018).
4. B. L. Henke, E. M. Gullikson, and J. C. Davis, "X-ray interactions: photoabsorption, scattering, transmission, and reflection at E = 50 − 30, 000 eV, Z = 1 − 92," *At. Data Nucl. Data* **54**, 181–342 (1993).
5. J. Jiang, D. De Simone, and G. Vandenberghe, "Difference in EUV photoresist design towards reduction of LWR and LCDU," *Proc. SPIE* **10146**, 101460A (2017).
6. J. Jiang, D. De Simone, and G. Vandenberghe, "Metal sensitizer in chemically amplified EUV resist: a study of sensitivity enhancement and dissolution," *J. Photopolym. Sci. Technol.* **30**(5), 591–597 (2017).
7. C. D. Higgins et al., "Resolution, line-edge roughness, sensitivity trade-off, and quantum yield of high photo acid generator resists for extreme ultraviolet lithography," *Jpn. J. Appl. Phys.* **50**, 036504 (2011).
8. Y. Vesters et al., "Sensitizers in EUV chemically amplified resist: mechanism of sensitivity improvement," *Proc. SPIE* **10583**, 1058307 (2018).
9. E. Gullikson, "Filter transmission," online tool from the Center for X-ray Optics (CXRO) at Berkeley Lab (LBNL), http://henke.lbl.gov/optical_constants/filter2.html.
10. G. F. Lorusso et al., "The need for LWR metrology standardization: the IMEC roughness protocol," *Proc. SPIE* **10585**, 105850D (2018).
11. A. Shehzad et al., "Photoresist absorption measurement at EUV wavelength by thin film transmission method," *J. Vac. Sci. Technol. B*, submitted.
12. A. Vaglio Pret et al., "Characterizing and modeling electrical response to light for metal-based EUV photoresists," *Proc. SPIE* **9779**, 977906 (2016).
13. P. de Schepper et al., "XAS photoresists electron/quantum yields study with synchrotron light," *Proc. SPIE* **9425**, 942507 (2015).
14. D. De Simone et al., "Exploring the readiness of EUV photo materials for patterning advanced technology nodes," *Proc. SPIE* **10143**, 101430R (2017).
15. H. Yamamoto et al., "Polymer structure dependence of acid generation in chemically amplified EUV resists," *Jpn. J. Appl. Phys.* **46**(7), L142–L144 (2007).
16. R. Hirose et al., "Dependence of absorption coefficient and acid generation efficiency on acid generator concentration in chemically amplified resist for extreme ultraviolet lithography," *Jpn. J. Appl. Phys.* **46**(40), L979–L981 (2007).
17. H. Yamamoto et al., "Proton dynamics in chemically amplified electron beam resist," *Jpn. J. Appl. Phys.* **43**, L848 (2004).
18. H. Yamamoto et al., "Polymer screening method for chemically amplified electron beam and X-ray resists," *Jpn. J. Appl. Phys.* **43**, 3971–3973 (2004).
19. Y. Vesters, D. De Simone, and S. De Gendt, "Dissolution rate monitor tool to measure EUV photoresist dissolution," *J. Photopolym. Sci. Technol.* **30**(6), 675–681 (2017).
20. H. Yamamoto, T. Kozawa, and S. Tagawa, "Study on dissolution behavior of polymer-bound and polymer-blended photo acid generator (PAG) resist by using quartz crystal microbalance (QCM) method," *Microelectron. Eng.* **129**, 65–69 (2014).

21. D. Joseph et al., "Chemical shift of Mn and Cr K-edges in X-ray absorption spectroscopy with synchrotron radiation," *Bull. Mater. Sci.* **36**(6), 1067–1072 (2013).
22. C. A. Mack, "Development of positive photoresists," *J. Electrochem. Soc.* **134**(1), 148–152. (1987).

Yannick Vesters received his BS and MS degrees in chemical engineering and material science from the University of Louvain-la-Neuve, Belgium. He worked as an engineer for two years before starting a PhD at the University of Leuven, Belgium. Currently, he is performing his PhD research on the improvement of the lithographic performances of photoresists for EUV lithography at imec. He focuses on the understanding of patterning mechanisms and on novel photoresist materials.

Biographies of the other authors are not available.